EurJIC
European Journal of Inorganic Chemistry

Research Article
doi.org/10.1002/ejic.202400207

Chemistry Europe
European Chemical Societies Publishing

www.eurjic.org

# 2-Pyridinyl/quinolyl-phenylamino-quinoline Complexes With CF3 and C2F5 Ligated Ni

Katja S. Håheim[+],[a] Shubham Deolka[+],[b] Robert R. Fayzullin,[c] Bjarte Aarmo Lund,[d] Eugene Khaskin,*[b] and Magne O. Sydnes*[a]

A new ligand architecture based on quinoline/pyridine attached *ortho* to the amine functionality on an aniline, which is coupled to another quinoline unit has been prepared. Ligands **L1** and **L2** have been complexed with $CF_3$ and $C_2F_5$ ligated nickel centers. The resulting complexes have been extensively studied by NMR spectroscopy (on $^{1}H$, $^{13}C\{^{1}H\}$, and $^{19}F$ nuclei) and single-crystal X-ray crystallography. A poorly defined mixture of complexes obtained from **L1** and nickel bis-trifluoromethyl complex was moderately active in C–H trifluoromethylation with the Umemoto I reagent.

## Introduction

C–H bond functionalization has become an immensely powerful tool in organic chemistry.[1] Strategies for C–H activation have to overcome two fundamental obstacles. The first challenge is the inherent stability of most C–H bonds, rendering them typically unreactive, and the second is controlling site selectivity in large molecules containing multiple and diverse C–H bonds.[2] New catalysts and approaches for C–H activation are thus an intensive focus of current research. In recent years, C–H activation has shown promise for the late-stage fluorination/trifluoromethylation of complex molecules, such as late-stage pharmaceutical intermediates or final drug compounds.[3] Fluorinated analogues of these compounds may give a new drug with the same basic mode of action, but with improved metabolic and activity profiles. Metal catalysts, including nickel, have been found to selectively modify such molecules, often in low yields, and with high metal loading. However, the approach creates a new drug analogue that can be purified and tested rapidly, and the costs of the organic drug molecule often outweigh that of the catalyst and the purification procedure. The addition of a $CF_3$ group to even a large molecule can dramatically alter the polarity and other physical properties, so the main goal of C–H trifluoromethylation is to have a selective process that is able to convert the starting material to a single product with high yield, potentially simplifying a difficult purification procedure. At least at the drug/molecule discovery stage, the goal of nickel catalyzed trifluoromethylation is to optimize selectivity and not necessarily turnover number (TON). As the reaction proceeds via a radical mechanism and the ligand parameters affecting catalytic activity are not well known, we often test new types of ligand systems for C–H trifluoromethylation.

Previously, our group has used high-valent nickel with naphthyridine ligands as catalysts for the light-mediated catalytic trifluoromethylation of various aryl and (het)aryl compounds (Figure 1).[4] The presence of an aromatic N-heterocycle with two fused aromatic rings likely played an important role in producing complexes that absorb visible light and undergo light-induced bond homolysis. The naphthyridine can also act as either a bidentate or monodentate ligand, and the slippage between the coordination modes might play a role in catalysis, with naphthyridine de-coordina-

[a] *K. S. Håheim,[+] M. O. Sydnes*
*Department of Chemistry, Bioscience and Environmental Engineering, University of Stavanger, NO-4036 Stavanger, Norway*
*E-mail: magne.o.sydnes@uis.no*

[b] *S. Deolka,[+] E. Khaskin*
*Okinawa Institute of Science and Technology Graduate University, Tancha, Onna-son, 904-0495 Okinawa, Japan*
*E-mail: eugenekhaskin@oist.jp*

[c] *R. R. Fayzullin*
*Arbuzov Institute of Organic and Physical Chemistry, FRC Kazan Scientific Center of RAS, 8 Arbuzov Street, Kazan 420088, Russian Federation*

[d] *B. A. Lund*
*Department of Chemistry, UiT The Arctic University of Norway, NO-9037, Tromsø, Norway*

[+] *These authors contributed equally to the work*

*Supporting information for this article is given available on the WWW under https://doi.org/10.1002/ejic.202400207*



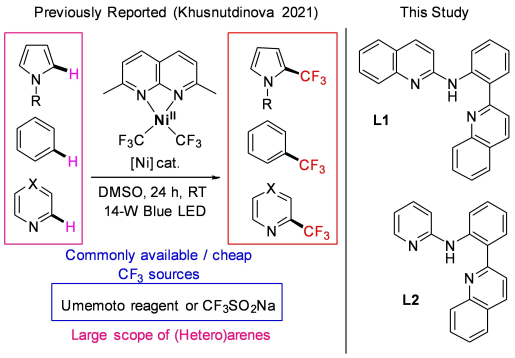


**Figure 1.** Previously reported catalytic trifluoromethylation with naphthyridine and ligands used in this study.

Research Article
doi.org/10.1002/ejic.202400207



tion and help in proton abstraction being identified as possible secondary roles of this ligand in the catalytic cycle. In a similar way, we envisioned **L1** and **L2**, with the possibility of a third coordination site, as dynamic ligands that can participate in both of these roles and allow for late-stage catalytic trifluoromethylation by allowing isomerization that leads to reactive intermediates, while proton abstraction is carried out by the uncoordinated third nitrogen: i.e. a pendant Lewis base (Figure 2).

In the current study, we explored a new NNN tridentate ligand motif where a pyridine/quinoline ring is located *ortho* to an amine functionality, that is coupled with a second distal quinoline unit for the purpose of testing nickel complexes in trifluoromethylation catalysis (Figure 1). While 2-aminopyridine or 2,2′-bipyridine-6,6′-diamine ligands are well known, the addition of a third donor connected via a conjugated linker gave a ligand backbone that proved to be, to the best of our knowledge, unused in organometallic chemistry, but that could lead to ligand-assisted substrate activation (Figure 2). When exploring the basic quinoline unit ligand motif **L1**, we were surprised to find hardly any reports in the literature on the basic skeletal arrangement of the rings as either a similar structure or a larger substructure, besides a synthetic paper where a related compound was synthesized in low yield.[5] However, compounds with the same basic connectivity, but with both quinolines replaced by pyridines do appear in a large number of industrial patents as parts of medicinal chemistry libraries,[6] or as parts of larger molecules used as components for light emitting diodes.[7]

Besides the paucity of previous reports on such a simple ligand motif, there were several other reasons for testing these ligands in catalysis. The amine *ortho* to the aromatic ring can participate in metal/ligand cooperation when bound to the pyridine via dearomatization, a process that can help in the activation of substrates where the metal coordinates the deprotonated substrate and the hydrogen atom is transferred to the ligand (as in Figure 2 bottom), which is then re-aromatized.[8] This dearomatization/re-aromatization is typically known to occur for *ortho* and *para* amino pyridines. The distal quinoline can play a role as an alternative 2 electron donor for the metal, leading to isomerization between several possible coordination compounds, or it can affect the second coordination sphere during catalysis.[9] Finally, the π-system of the quinoline can act as an electron acceptor, that may be able to stabilize the high-valent nickel (III)/(IV) intermediates, something that was observed in ligands with a similar electronic profile.[10]

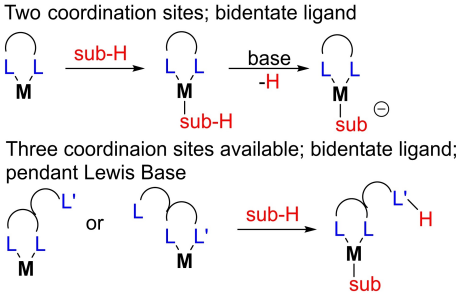


**Figure 2.** Possible coordination modes of **L1** and **L2** with a metal center.

## Results and Discussion

### Ligand Synthesis

Our group has previously described the preparation of biaryl **1** through a Suzuki-Miyaura cross-coupling reaction,[11] which served as the starting material for the synthesis of the desired ligands **L1** and **L2**. Using a classical Buchwald-Hartwig amination reaction between biaryl **1** with either 2-bromoquinoline (**2a**) or 2-bromopyridine (**2b**) we obtained the desired compounds in 52 and 49% yield, respectively (Scheme 1). The ease with which these substrates are prepared suggests further modifications of this framework can be easily carried out.

In addition to ligands **L1** and **L2**, we have also prepared three more N,N,N quinoline/pyridine compounds, where **L3** is prepared in a similar manner to **L1** and **L2** (Scheme 2a). The two final ligands, viz. **L4** and **L5**, were prepared by reductive amination to avoid overalkylation. Starting from biaryl **1** and treating it with quinoline-2-carboxaldehyde in methanol using molecular sieves (4 Å) to remove water, we obtained the corresponding imine as evident from TLC-LRMS analysis. Then, a reduction was carried out using $NaBH_3CN$ to give **L4** in 78% yield. For the synthesis of **L5**, $NaBH_4$ was sufficient to give the target **L5** in 68% yield (Scheme 2b).

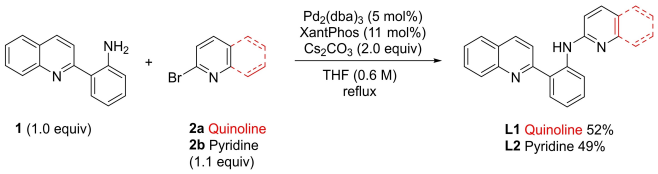


**Scheme 1.** Synthesis of ligands **L1** and **L2** using a Buchwald-Hartwig amination reaction.

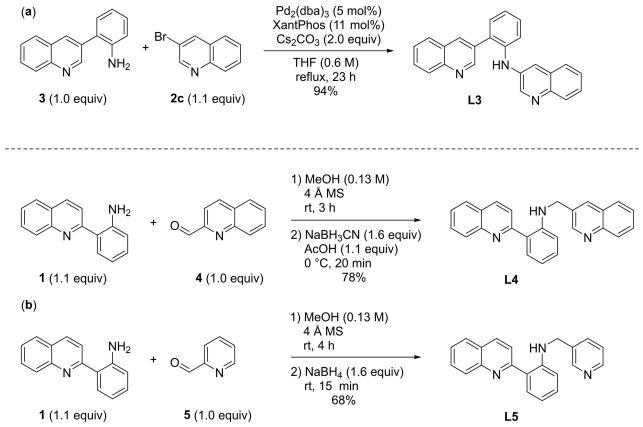


**Scheme 2.** Preparation of ligands **L3**-**L5**.

Research Article
doi.org/10.1002/ejic.202400207





### Organometallic Complexation

With ligands **L1**-**L5** in hand we attempted the complexation of electron-poor Ni(II) precursors. Right away it was clear that **L3**-**L5**, which display different connectivity not amenable to bidentate binding, are not within the scope of the current work where we attempted to isolate well-defined, single metal species. As expected, **L3**-**L5**, as observed in preliminary experiments, are more amenable to multi-metallic/multi-isomeric structures that are difficult to separate and study; further work with them was thus not pursued. A quinoline/pyrdine analogue of **L3** was not prepared due to these initial observations.

### Complexation with L1

The presence of several isomers of complexes with **L1** and **L2** was always a potential problem as the ligands have a few potential bidentate binding modes. The reaction between **L1** and the nickel precursor $(CH_3CN)_2Ni(CF_3)_2$ led to a mixture of three complexes (i.e. three pairs of equally integrating $CF_3$ peaks in the $^{19}F$ NMR spectrum) and a complicated mixture of these three species in the $^{1}H$ NMR spectrum (Scheme 3; Figures S11—S14). These are all the three isomers possible upon bidentate binding of the nickel complex. Due to the lack of symmetry between the $CF_3$ groups, six peaks can be observed in the $^{19}F$ NMR −26 to −29 ppm region. These shifts are in the range of typical Ni(II)-$CF_3$ peaks and **L1Ni(CF$_3$)$_2$** can be said to exist as an unequal mixture of three isomers.[12] Interestingly, and as discussed in more detail below, the $CF_3$ peaks appear as quartets due to long-range $^{4}J_{FF}$ coupling between the fluorines through the metal center. Due to an inability to isolate a single complex easily, resulting in eventual decomposition of the original three complexes to an unknown mixture upon prolonged crystallization attempts, the crude reaction mixture was not worked up further.

We decided to use a more sterically hindered Ni precursor with **L1** in an attempt to obtain a single organometallic species. The reaction between **L1** and $(CH_3CN)_2Ni(CF_2CF_3)_2$ led to a single complex **L1Ni(C$_2$F$_5$)$_2$** that could be isolated and crystallized (Figure 3). The complex proved stable under $N_2$ atmosphere. In the solid state, complex **L1Ni(C$_2$F$_5$)$_2$** (Figure 3) has a $C_{quin}$–$N_{imine}$ ($C_{31}$–$N_2$) and $C_{benz}<C->N_{imine}$ ($C_{21}$–$N_2$) bond lengths of 1.298(2) and 1.428(2) Å respectively, indicative of a clear-cut, dearomatized structure. The NH hydrogen atom was located from the electron density map. The Ni–$N_{imine}$ and Ni–$N_{quin}$ bond lengths are 1.942(2) and 1.962(2) Å and the Ni–C bond lengths *trans* to those respective nitrogens are 1.940(2) and 1.929(2) Å. While there is some variation in Ni–C bond lengths, it is minor and there is not much difference between the *trans* effect of the imine and quinoline nitrogens. The imine-adjacent carbon of the bridging Ph group is 2.57 Å away from the metal center, which is too far for a bonding interaction and the otherwise close distance likely just reflects the geometry of the ligand.

Despite the single isomer in the solid-state, in the NMR spectra the signals are slightly broadened, and they do not resolve even at low temperature. While in the $^{1}H$ NMR spectrum all the aromatic signals are accounted for, the broadening makes it difficult to accurately record coupling between the protons (Scheme S15). The $^{13}C\{^{1}H\}$ NMR peaks are slightly broadened, but all 24 resonances can be located, with the $C_2F_5$ carbon peaks not being observed due to extensive $J_{CF}$ coupling (Scheme S16). The broadening in both $^{1}H$ NMR and $^{13}C\{^{1}H\}$ NMR spectra may hint at rapid positional exchange between the groups. This intriguing possibility is confirmed by the observation of only two peaks in the $^{19}F$ NMR, despite the $C_2F_5$ groups being inequivalent (Figure S19). The lack of coupling between the $CF_3$ and $CF_2$ fluorines is a known effect that occurs between vicinal F atoms in polyfluoroalkyl species

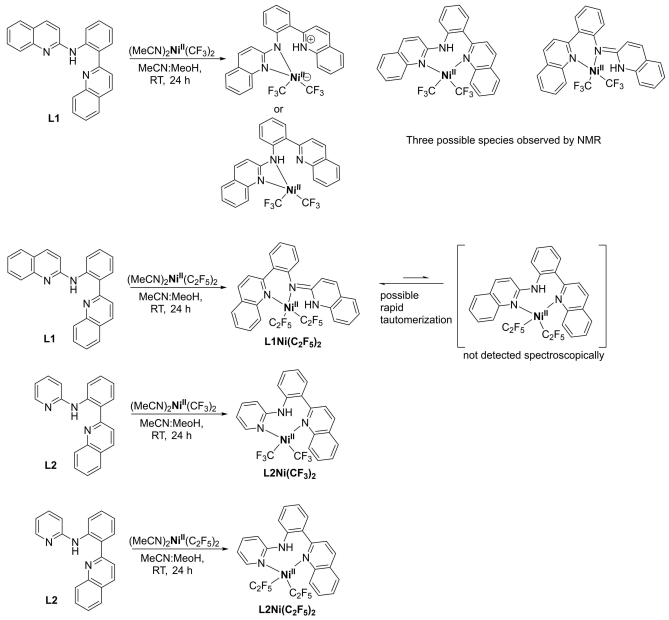


**Scheme 3.** Synthesis of complexes.

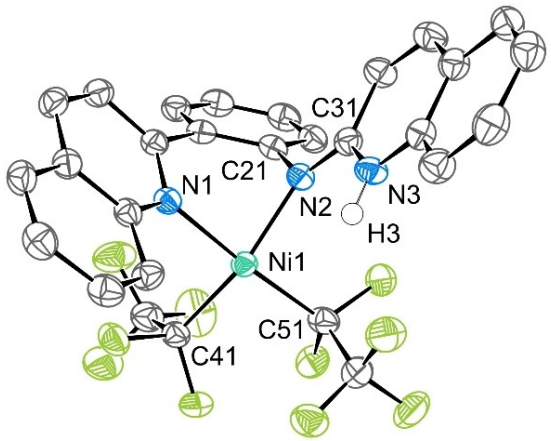


**Figure 3.** Molecular structure of **L1Ni(C$_2$F$_5$)$_2$** in the crystal with anisotropic displacement ellipsoids at the 70% probability level. All hydrogen atoms except for [N]H are omitted for clarity. Selected interatomic distances [Å]: Ni1–N1 1.9622(15), Ni1–N2 1.9422(15), Ni1–C41 1.9395(18), Ni1–C51 1.9292(19), N2–C21 1.428(2), N2–C31 1.298(2), N3–H3 0.86(3).

Research Article
doi.org/10.1002/ejic.202400207



so each resonance appears as a virtual singlet; this is believed to occur due to the rotational averaging of coupling constants of opposite sign between the $^3J_{FF}$ $CF_2$ and $CF_3$ groups.[13] In complexes of nickel and cobalt with pentafluoroethyl groups, a similar effect is observed.[14] However, when multiple $C_2F_5$ groups are inequivalent, usually two sets of signals are observed and in fact we should be able to observe $^4J_{FF}$ coupling through the metal center.[15] In the $^{19}F$ NMR of **L1Ni($C_2F_5$)$_2$** we never get a good resolution of the single set of peaks even at lower temperatures and the expected $^4J_{FF}$ coupling is also not seen. We lean towards an explanation that rapid imine decoordination and re-coordination occurs, thus the $C_2F_5$ signals are averaged on the NMR timescale.

### Complexation with L2

In comparison to **L1**, ligand **L2** has the proximal quinoline unit replaced by a pyridine and the corresponding coordination chemistry may thus be affected by the steric and electronic differences. Reacting **L2** with both the $CF_3$ and the $CF_3CF_3$ nickel precursors gave single complexes that could be isolated and characterized by NMR spectroscopy and single crystal X-ray diffraction.

The reaction between **L2** and $(CH_3CN)_2Ni(CF_3)_2$ gave a highly stable complex that did not show any sign of decomposition upon workup, unlike the reaction with **L1**, hinting at a rich organometallic chemistry that may be accessed by slight changes in the ligand backbone. In the resulting **L2Ni($CF_3$)$_2$** complex (Figure 4), the metal is bound through the quinoline and pyridine nitrogens while the amine remains unbound. The topology of the complex is accordingly drastically different compared to **L1Ni($C_2F_5$)$_2$**. The bridging phenyl ring sits above the metal plane, with the closest Ni–C distances being 2.80 and 3.02 Å. The phenyl ring may act to block that face of the metal, perhaps preventing further reactivity. The complex is diamagnetic, as is expected for a square planar Ni(II) species. $C_{pyr}$–$N_{amine}$ ($C_{31}$–$N_2$) and $C_{benz}$–$N_{amine}$ ($C_{21}$–$N_2$) bond lengths are 1.372(6) and 1.418(5) Å respectively, with the substitution of pyridine for quinoline effectively acting to favor the non-dearomatized isomer. The Ni–C bonds are both close to, and just above 1.9 Å in length, characteristic of both being *trans* to $sp^2$ hybridized N donors.

The $^{19}F$ NMR spectrum shows two singlet $CF_3$ peaks at −27.4 and −28.9 ppm, typical shifts for $CF_3$ fluorines. Unlike the $^{19}F$ NMR spectrum of the three isomers of **L1Ni($CF_3$)$_2$**, the signals are not quartets, showing a lack of $^4J_{FF}$ coupling or of a fast exchange between the $CF_3$ groups (Figure S27). All 14 aromatic H resonances are well resolved in the $^1H$ NMR (Figure S23), with the NH amine proton being located at 6.33 ppm. 20 resonances are observed in the $^{13}C\{^1H\}$ NMR spectrum (Figure S24), with the $CF_3$ groups below the signal to noise ratio due to $J_{CF}$ coupling (see Figure S18). After prolonged standing in solution, **L2Ni($CF_3$)$_2$** also begins to slowly decompose and new minor peaks appear in the $^{19}F$ NMR in the −80 to −150 region, however the complex is stable in the solid state and the decomposition is much slower compared to what was observed for **L1Ni($CF_3$)$_2$**.

Reacting $(MeCN)_2Ni^{II}(CF_2CF_3)_2$ with **L2** gave complex **L2Ni($C_2F_5$)$_2$** (Figure 5), which is very similar to **L2Ni($CF_3$)$_2$** and has the exact same binding mode and tautomeric form of the ligand. The Ni–C bond distances are 1.948(2) and 1.958(2) Å for the carbon atoms *trans* to the N-heterocycles. The nickel nitrogen distances are: for the pyridine ($N_3$–Ni 1.976(2) Å), and for the quinoline nitrogen ($N_1$–Ni 1.958(2) Å). Since a direct comparison can be made with **L2Ni($CF_3$)$_2$** due to similar bonding, the most pertinent and unusual difference observed is that all four donor atoms are at longer distances when compared to the $CF_3$ complex, which could be due to the greater steric constraints imposed by a bigger $C_2F_5$ group.

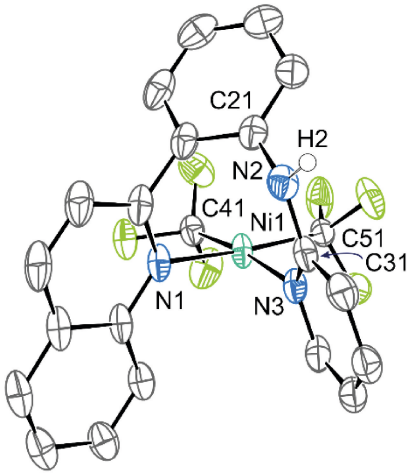


**Figure 4.** Molecular structure of **L2Ni($CF_3$)$_2$** in the crystal with anisotropic displacement ellipsoids at the 50% probability level. All hydrogen atoms except for [N]H, the co-crystallized benzene molecule, and the minor disorder component are omitted for clarity. Selected interatomic distances [Å]: Ni1–N1 1.9457(16), Ni1–N3 1.9638(17), Ni1–C41 1.907(2), Ni1–C51 1.914(3), N2–C21 1.419(3), N2–C31 1.374(3), N2–H2 0.88(3).

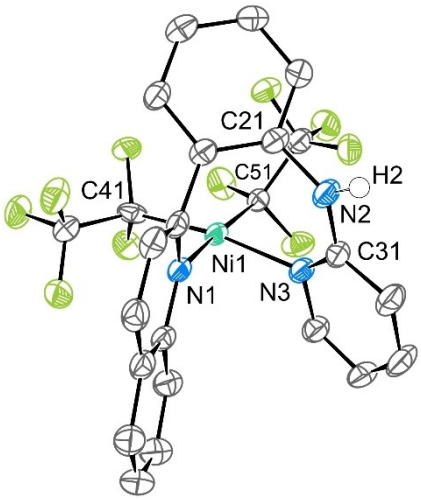


**Figure 5.** Molecular structure of **L2Ni($C_2F_5$)$_2$** in the crystal with anisotropic displacement ellipsoids at the 70% probability level. All hydrogen atoms except for [N]H are omitted for clarity. Selected interatomic distances [Å]: Ni1–N1 1.9578(17), Ni1–N3 1.9756(16), Ni1–C41 1.948(2), Ni1–C51 1.9577(19), N2–C21 1.429(2), N2–C31 1.363(3), N2–H2 0.91(3).

Research Article
doi.org/10.1002/ejic.202400207



It is interesting to compare the NMR spectra of **L2Ni($C_2F_5$)$_2$** to **L1Ni($C_2F_5$)$_2$** as in the latter complex, both $C_2F_5$ groups are equivalent due to rapid exchange. However, in the former complex, the $^1$H NMR (Figure S32) and $^{13}$C{$^1$H} NMR (Figure S33) spectra are well resolved and coupling data can be easily extracted (except for the $C_2F_5$ carbon atoms due to low intensity after CF coupling). Two of the aromatic carbon resonances are split into a doublet by a single fluorine, suggesting that the $CF_2$ fluorines are not magnetically equivalent. In fact, in the $^{19}$F NMR, the $^4J_{FF}$ coupling through the metal center that we earlier observed in cobalt is well seen.[15] Each $CF_2$ fluorine is magnetically inequivalent and is split into a doublet or a doublet of doublets/multiplets. There is also residual coupling to one of the $CF_3$ groups. The spectrum expansion of the $CF_2$ region (Figure S36), showing two inequivalent $C_2F_5$ groups on a Ni(II) center, is reproduced below (Figure 6).

## Catalysis

We tested the mixture of **L1** and the $(CH_3CN)_2Ni(CF_3)_2$ precursor in trifluoromethylation catalysis with an Umemoto (Compound **A**, Scheme 4) and a Togni reagent (1-trifluoromethyl-1,2-benziodoxol-3(1H)-one) with four heterocycles. We quickly observed that unlike other systems reported by us,[16] only the Umemoto reagent showed acceptable TONs, hinting that the reaction likely proceeds by an electrophilic pathway. This limits us to only using the $CF_3$ group in the catalytic reactions since other Umemoto reagents with different fluoroalkyl substituents are not readily available. Four representative electron-rich heterocycles were trifluoromethylated in acceptable yields using the protocol below (Scheme 4).

The use of complex **L2Ni($CF_3$)$_2$** gave inferior results in initial experiments with substrate **a**, so its use was not pursued. The catalysis likely proceeds better with the mixture of three possible complexes (i.e. **L1Ni($CF_3$)$_2$** ; see SI) due to more facile de-coordination and isomerization between the complexes. Unlike our earlier report with the Umemoto reagent and the naphthyridine ligand, light was not required for the reaction.[4] With that naphthyridine ligand however, a control reaction without the use of blue LED gave $<5\%$ yield of the product. Subsequently we published on a "ligand-free" (i.e. acetonitrile or DMSO solvent served as ligands) system that is able to use the Togni reagent as a two electron oxidant, without the aid of light, and where we were not able able to detect Ni(IV).[16b] It is still likely that a transient Ni(IV) forms based on a paper we published a year later where a specialized electron poor, bidentate fluoroalkyl ligand was required for the detection of this transient Ni(IV) species. This suggests that it may be possible to form Ni(IV) under similar reaction conditions with any electron poor suitable/similar nitrogen donor ligand system.[16a] Thus, it is likely that de-coordination of one of the arms or **L1** could allow for 2e$^-$ oxidation access to Ni(IV). Finally, the use of Umemoto reagent II (2,8-diflouro-S-(trifluoromethyl)dibenzothiophenium salt) in catalysis with nickel complexes without the use of light has been reported to proceed via a Ni(IV) intermediate.[12,17]

Thus, by analogy with our earlier published work and that of others, a likely mechanism involves oxidation to Ni(IV) via the Umemoto reagent (Scheme 5). Subsequent homolytic cleavage generates a fluoroalkyl radical and a Ni(III) center.

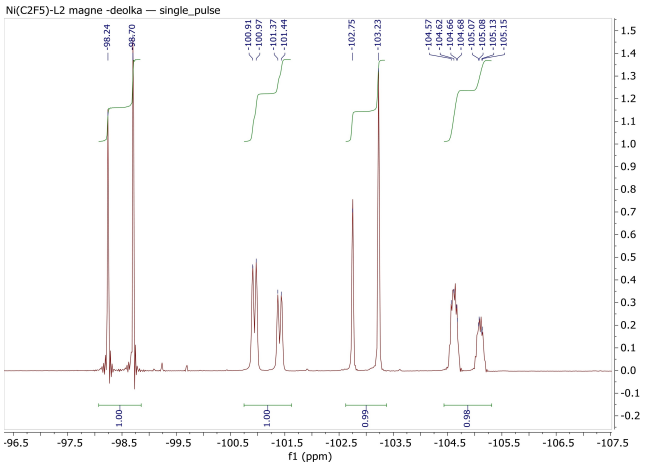


**Figure 6.** $^{19}$F NMR spectrum expansion of **L2Ni($C_2F_5$)$_2$** in THF-$d_8$ displaying $^4J_{FF}$ coupling of the magnetically inequivalent fluorine atoms of the $CF_2$ groups.

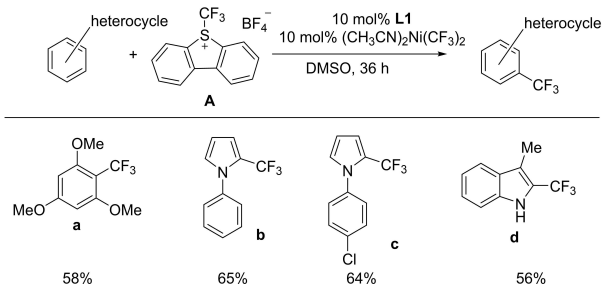


**Scheme 4.** Catalytic trifluoromethylation with the Umemoto I (**A**) reagent.

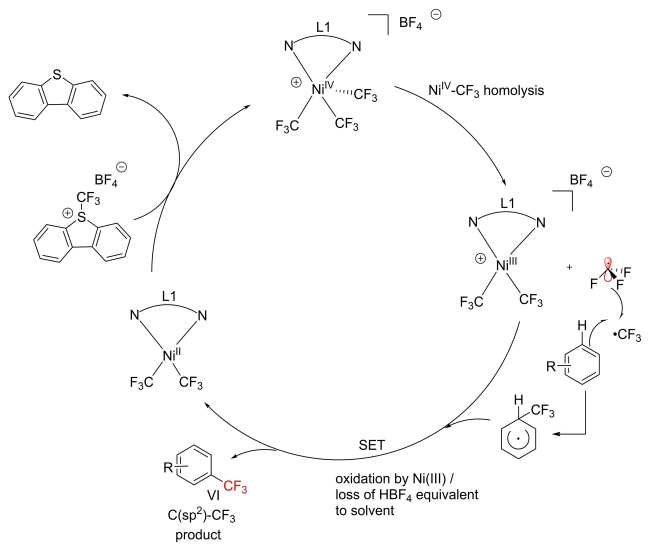


**Scheme 5.** Trifluoromethylation catalysis results with a mixture of **L1** and nickel precursor.

Research Article
doi.org/10.1002/ejic.202400207





Reaction of the fluoroalkyl radical with the substrate generates a radical adduct, which is reduced by the Ni(III) center (see Figure 2 for the possible role of the third ligand arm) to generate Ni(II) and the functionalized substrate.

To the best of our knowledge, the best nickel catalyzed alkylfluorination system has earlier been reported by us,[16b] where any fluoroalkyl Togni reagent can be used with the same catalyst, allowing for yields of up to 90%, with the ability to insert any $C_xF_{2x+1}$ or aryl-$CF_2CF_2$ units via CH activation, into a broad range of electron-rich substrates that include peptides. The current system is only applicable to the $CF_3$ moiety and the more expensive Umemoto reagent, so despite the interesting ligand architecture, it is inferior in fluoroalkylation catalysis.

## Conclusions

We synthesized a number of nickel fluoroalkyl complexes supported by two novel quinoline based ligands. As the ligands had unusual connectivity that has not been well explored in organometallics, we wanted to establish whether they could act as competent ligands in a well-described system, and to see if the subsequent complexes could be used for catalysis.

As expected, the identity of the final complex depended on the nature of the fluoroalkyl substituent and on the ligand. One of the well-defined complexes that formed with the $Ni(CF_3)_2$ precursor and **L2** was unfortunately not active in trifluoromethylation catalysis; however, a poorly defined mixture of complexes that was obtained by the use of **L1** and a nickel bis trifluoromethyl complex was moderately active in C–H trifluoromethylation with the Umemoto I (**A**) reagent. Activity in catalysis may depend on the ability of the metal to convert between several isomers in solution, and thus ligands of the same basic architecture can be explored as an additive in catalytic reactions with electron-rich metal precursors or with metal salts in the future. Interestingly, the difference between the **L1** quinoline and **L2** pyridine based ligands results in different tautomers in the $Ni(C_2F_5)_2$ complexes as the result of the proton residing on either the quinoline **L1**, or the amine as in the case of **L2.**

## Supporting Information Summary

Experimental section, including ligand and complex synthesis including their NMR spectra, and HRMS/IR/UV-vis spectra and general X-ray data, as well as catalytic experiments including their $^{19}F$ NMR spectra, are available in the SI. Deposition Numbers https://www.ccdc.cam.ac.uk/services/structures?id=doi:10.1002/ejic.2024002072299911 (for **L2Ni($CF_3$)$_2$**), 2299912 (for **L1Ni($C_2F_5$)$_2$**), 2299913 (for **L2Ni($C_2F_5$)$_2$**), 2299914 (for **L1**) contain the supplementary crystallographic data for this paper. These data are provided free of charge by the joint Cambridge Crystallographic Data Centre and Fachinformationszentrum Karlsruhe http://www.ccdc.cam.ac.uk/structures Access Structures service.

The authors have cited additional references within the Supporting Information.[14b,18,19]

## Acknowledgements

Okinawa Institute of Science and Technology is gratefully acknowledged for funding. OIST Instrumental Analysis Support (IAS) and the Engineering Section are acknowledged for technical support. Funding from Universitetsfondet and the ToppForsk program at University of Stavanger is gratefully acknowledged. Thanks are also due to Scandinavia-Japan Sasakawa Foundation for financing a research stay for M.O.S. in the Khaskin group at OIST. R.R.F. performed crystal structure determination within the government assignment for the FRC Kazan Scientific Center of RAS.

## Conflict of Interests

The authors declare no conflict of interest.

## Data Availability Statement

The data that support the findings of this study are available in the supplementary material of this article. These include descriptions of ligand and complex synthesis; catalytic procedures; NMR data; ATR-IR; UV-Vis; ESI-(HR)MS, and Xray data.

**Keywords:** Nickel · Trifluoromethylation · Catalysis · Quinoline · Complexation

[1] J. Wencel-Delord, F. Glorius, *Nat. Chem.* **2013**, *5*, 369–375.
[2] a) D. Leow, G. Li, T.-S. Mei, J.-Q. Yu, *Nature* **2012**, *486*, 518–522; b) Y.-J. Liu, H. Xu, W.-J. Kong, M. Shang, H.-X. Dai, J.-Q. Yu, *Nature* **2014**, *515*, 389–393.
[3] a) S. Barata-Vallejo, B. Lantaño, A. Postigo, *Chem. Eur. J.* **2014**, *20*, 16806–16829; b) H. Baguia, G. Evano, *Chem. - Eur. J.* **2022**, *28*, e202200975; c) P. P. Singh, P. K. Singh, V. Srivastava, *Org. Chem. Front.* **2023**, *10*, 216–236.
[4] S. Deolka, R. Govindarajan, E. Khaskin, R. R. Fayzullin, M. C. Roy, J. R. Khusnutdinova, *Angew. Chem. Int. Ed.* **2021**, *60*, 24620–24629.
[5] N. P. Peet, S. Sunder, R. J. Barbuch, M. R. Whalon, E. W. Huber, J. C. Huffman, *J. Heterocycl. Chem.* **1989**, *26*, 1611.
[6] a) N. Buschmann, R. A. Fairhurst, P. Furet, T. Knoepfel, C. Leblanc, R. Mah, WO2016151499, **2016**; b) C. Sun, P. Gao, L. Liu, R. Bao, CN109745321, **2019**; c) A. C. Castro, WO2020243415, **2020**; d) A. C. Castro, M. Burke, WO2022120355, **2022**; e) A. C. Castro, M. Burke, B. Amidon, H. Frosch, WO2022159986, **2022**; f) Y. Kang, I. Lee, B. Yoo, J. D. Kim, Y. Choi, S. Ha, A. Kwon, J. S. Park, WO2023136645, **2023**.
[7] a) J. T. Je, S. U. Jung, N. I. Kim, S. H. Lee, KR2011057078, **2011**; b) J. Lee, S. Kim, B. Park, S. Lee, S. Hong, Y. Kwak, O. Kwon, US20180342686, **2018**; c) G. Deng, Y. Zhao, Z. Chen, J. Wang, CN112500298, **2021**.
[8] J. R. Khusnutdinova, D. Milstein, *Angew. Chem. Int. Ed.* **2015**, *54*, 12236–12273.
[9] S. Deolka, N. Tarannam, R. R. Fayzullin, S. Kozuch, E. Khaskin, *Chem. Commun.* **2019**, *55*, 11350–11353.
[10] K. D. Spielvogel, N. C. Stumme, T. V. Fetrow, L. Wang, J. A. Luna, J. M. Keith, S. K. Shaw, S. R. Daly, *Inorg. Chem.* **2022**, *61*, 2391–2401.

[11] a) K. S. Haaheim, I. T. Urdal Helgeland, E. Lindback, M. O. Sydnes, *Tetrahedron* **2019**, *75*, 2949–2957; b) K. S. Haaheim, E. Lindback, K. N. Tan, M. Albrigtsen, I. T. U. Helgeland, C. Lauga, T. Matringe, E. K. Kennedy, J. H. Andersen, V. M. Avery, M. O. Sydnes, *Molecules* **2021**, *26*, 3268; c) K. S. Haaheim, B. A. Lund, M. O. Sydnes, *Eur. J. Org. Chem.* **2023**, *26*, e202300137.
[12] S. T. Shreiber, D. A. Vicic, *Angew. Chem. Int. Ed.* **2021**, *60*, 18162–18167.
[13] a) R. E. Graves, R. A. Newmark, *J. Chem. Phys.* **1967**, *47*, 3681; b) R. A. Newmark, *J. Fluorine Chem.* **2009**, *130*, 389–393.
[14] a) V. N. Madhira, P. Ren, O. Vechorkin, X. Hu, D. A. Vicic, *Dalton Trans.* **2012**, *41*, 7915–7919; b) C.-P. Zhang, H. Wang, A. Klein, C. Biewer, K. Stirnat, Y. Yamaguchi, L. Xu, V. Gomez-Benitez, D. A. Vicic, *J. Am. Chem. Soc.* **2013**, *135*, 8141–8144; c) S. T. Shreiber, J. J. Scudder, D. A. Vicic, *Organometallics* **2019**, *38*, 3169–3173; d) S. T. Shreiber, D. A. Vicic, *J. Organomet. Chem.* **2021**, *949*, 121974; e) T. Xue, S. T. Shreiber, R. E. Cramer, D. A. Vicic, *J. Fluorine Chem.* **2022**, *261–262*, 110030.
[15] H. M. Dinh, R. Govindarajan, S. Deolka, R. R. Fayzullin, S. Vasylevskyi, E. Khaskin, J. R. Khusnutdinova, *Organometallics* **2023**, *42*, 2632–2643.
[16] a) S. Deolka, R. Govindarajan, S. Vasylevskyi, M. C. Roy, J. R. Khusnutdinova, E. Khaskin, *Chem. Sci.* **2022**, *13*, 12971–12979; b) S. Deolka, R. Govindarajan, T. Gridneva, M. C. Roy, S. Vasylevskyi, P. K. Vardhanapu, J. R. Khusnutdinova, E. Khaskin, *ACS Catal.* **2023**, *13*, 13127–13139.
[17] E. A. Meucci, S. N. Nguyen, N. M. Camasso, E. Chong, A. Ariafard, A. J. Canty, M. S. Sanford, *J. Am. Chem. Soc.* **2019**, *141*, 12872–12879.
[18] a) G. M. Sheldrick, *Acta Crystallogr. Sect. A Found. Adv.* **2015**, *71*, 3–8; b) G. M. Sheldrick, *Acta Crystallogr. Sect. C Struct. Chem.* **2015**, *71*, 3–8.
[19] L. J. Farrugia, *J. Appl. Crystallogr.* **2012**, *45*, 849–854.

Manuscript received: April 12, 2024
Revised manuscript received: June 14, 2024
Accepted manuscript online: June 21, 2024
Version of record online: August 21, 2024